Multiple diffusive behaviors of the random walk in inhomogeneous environments

Xiao Luo,* Jing-Dong Bao, and Wen-Yue Fan
Department of Physics, Beijing Normal University, Beijing 100875, People's Republic of China

(Received 21 July 2023; accepted 20 December 2023; published 22 January 2024)

Anomalous diffusive behaviors are observed in highly inhomogeneous but relatively stable environments such as intracellular media and are increasingly attracting attention. In this paper we develop a coupled continuous-time random walk model in which the waiting time is power-law coupled with the local environmental diffusion coefficient. We provide two forms of the waiting time density, namely, a heavy-tailed density and an exponential density. For different waiting time densities, anomalous diffusions with the diffusion exponent between 0 and 2 and Brownian yet non-Gaussian diffusion can be realized within the present model. The diffusive behaviors are analyzed and discussed by deriving the mean-squared displacement and probability density function. In addition we derive the effective jump length density corresponding to the decoupled form to help distinguish the diffusion types. Our model unifies two kinds of anomalous diffusive behavior with different characteristics in the same inhomogeneous environment into a theoretical framework. The model interprets the random motion of particles in a complex inhomogeneous environment and reproduces the experimental results of different biological and physical systems.

DOI: 10.1103/PhysRevE.109.014130

I. INTRODUCTION

Research on the diffusion of tracer particles in a fluid goes back to the 19th century. After Robert Brown discovered the irregular random motion of pollen particles suspended in water in 1820 [1], many scientists began to study this phenomenon through experiments [2–4] and by determining the diffusion mechanisms [5–9]. Many experiments have revealed that the standard model of Brownian motion no longer satisfactorily describes all particle diffusive behaviors, and deviations from linear time dependence have been observed for a long time. Modern microscopic techniques have revealed that the mean-squared displacement (MSD) has an anomalous power-law time-dependence $\langle x^2(t)\rangle \simeq t^{\omega}$ with $0 < \omega < 1$ or $1 < \omega < 2$, called subdiffusion or superdiffusion, respectively. Such anomalous diffusions are common in the inhomogeneous environment of cells [10–17]. Subdiffusion generally occurs in the cytoplasm of living biological cells [18–20], artificially crowded liquids [21–23], and quasi-two-dimensional systems such as lipid bilayer membranes [24–28]. Superdiffusion is usually associated with active processes and is also observed in living cells [29,30]. One method for describing anomalous diffusions is the continuous-time random walk (CTRW) theory presented by Montroll [31] and Scher [32]. The CTRW is a typical phenomenological model characterized by the jump length ζ and the waiting time τ of a particle between two successive jumps, which are both drawn from a joint probability density function (PDF) $\psi(\zeta,\tau)$, where $\lambda(\zeta) = \int_0^{\infty} d\tau\,\psi(\zeta,\tau)$ is the jump length PDF and $P(\tau) = \int_{-\infty}^{\infty} d\zeta\,\psi(\zeta,\tau)$ is the waiting time PDF. To date, models based on the CTRW have successfully explained many anomalous diffusion mechanisms in physical, biological, and geological systems [33].

Recently, researchers have experimentally observed that cell membranes are composed of many stably distributed patches with different sizes and diffusion coefficients [34–38]. In such inhomogeneous environments, normal diffusion, subdiffusion, superdiffusion, and Brownian yet non-Gaussian diffusion are all observed [39–46]. The so-called Brownian yet non-Gaussian diffusion mentioned here is characterized by a linear growth in time of the MSD, yet the PDF of the particle displacement exhibits a Laplace shape at a short time, and after a longer time, it crosses over to a Gaussian profile. Obviously their diffusion mechanisms are different. There is a need for a theoretical model to describe these behaviors and reveal what causes them to exhibit completely different diffusive properties. Massignan *et al.* expressed the diffusive behavior mathematically by using a variable random diffusion coefficient [47]. Although their model can be used to explain only subdiffusion, it provides good inspiration for further research [48–50].

Different from the current Lévy walk model to describe the inhomogeneous environments [51], we develop a coupled CTRW model in which the waiting time τ has a power-law coupling with the local environmental diffusion coefficient $D(\tau)$ to demonstrate the environmental inhomogeneities. Through this coupling relationship, we further define the jump length density $\lambda(\zeta|\tau)$. We provide two forms of waiting time density $P(\tau)$, namely, a heavy-tailed density and an exponential density, which allows us to describe a broader range of physical phenomena. The numerical and analytical results show that different $P(\tau)$ lead to anomalous diffusive behaviors with completely different diffusive characteristics.

The remainder of this paper is structured as follows. In Sec. II we describe the model in detail and give calculation conclusions. In Secs. III and IV we analyze and discuss the anomalous diffusive behaviors for the heavy-tailed and exponential forms of $P(\tau)$, respectively. Section V presents our conclusions.

*202131140005@mail.bnu.edu.cn

II. THE COUPLED MODEL

We consider the case of noninteracting particles diffusing in one dimension. The particles are in an environment composed of many stably distributed patches with different sizes and diffusion coefficients. Each particle is located in its own patch and has an independent motion trajectory. We explain specifically the motion process for individual particles. Consider a particle that initially stays in a patch for a period τ_1, and then makes an instantaneous random jump ζ_1 to an adjacent patch and stays for another period τ_2, and then continues to jump to the next adjacent patch, and so on. We assume that each random jump always takes the particle from one patch to another adjacent one, and the waiting time τ is the time cost of this process.

Physically, if a particle spends a long waiting time τ in a patch, it may mean that the current medium density is high, and the particle diffusion ability is weak. A long τ is a manifestation of the high medium density. Correspondingly, a short τ indicates that the particle diffusion ability is strong. Based on the characteristics of the environment, we use the diffusion coefficient D as an indicator to describe the particle diffusion ability. It can be found that D is not independent of τ, but negatively correlated with it. Moreover, a large patch region may also lead to a long τ and usually has a larger diffusion coefficient than a small patch. For example, Kühn *et al.* used the fluorescent labeling method to research the diffusion coefficient of a freely diffusing model protein in fine cellular structures [36]. They found that compared with small structures such as the endoplasmic reticulum, Golgi apparatus, and mitochondria, proteins diffuse more easily in the cytoplasm that has a large region and have a longer motion time in it. Therefore, there may also be a positive correlation between $D(\tau)$ and τ.

For our present model in which τ is coupled with $D(\tau)$, we first confirm τ, which is drawn from the waiting time density $P(\tau)$. We provide two forms of $P(\tau)$, which are heavy-tailed and exponential, respectively. When $P(\tau)$ is heavy-tailed, it can read as

$$P(\tau) \simeq \sigma \tau^{-\sigma-1}, \quad 0 < \sigma < 2. \tag{1}$$

For the long time limit $t \to \infty$, its Laplace form is written as

$$P(u) = 1 - \Omega_\sigma u^\sigma, \quad 0 < \sigma < 1 \tag{2}$$

and

$$P(u) = 1 - \eta_\sigma u + \Omega_\sigma u^\sigma, \quad 1 < \sigma < 2, \tag{3}$$

in which $\Omega_\sigma = |\Gamma(1-\sigma)|$, $\eta_\sigma = \sigma/(\sigma-1)$. For $\sigma \in (0,1)$, the mean waiting time diverges, whereas if $\sigma \in (1,2)$, the mean waiting time is finite, but its variance still diverges. Actually, these two different ranges of σ will lead to $P(\tau)$ to display quite different properties [33]. When $P(\tau)$ is exponential, it can be expressed as

$$P(\tau) = \frac{1}{b}\exp\left(-\frac{1}{\mathrm{b}}\tau\right), \quad 0 < \mathrm{b}, \tag{4}$$

and the corresponding Laplace form is

$$P(u) \simeq 1 - bu. \tag{5}$$

The coupling relationship between $D(\tau)$ and τ can be described as $D(\tau) = a\tau^\alpha$ with $0 < a$ and $-1 < \alpha < 1$. Such a power-law coupling form could better demonstrate the environmental inhomogeneities.

Correspondingly, the particle jump length is sampled from a Gaussian-like function:

$$\lambda(\zeta|\tau) = \frac{1}{\sqrt{2\pi D(\tau)\tau}}\exp\left[\frac{-\zeta^2}{2\mathrm{D}(\tau)\tau}\right]. \tag{6}$$

Whenever a particle enters a new patch, its waiting time and next jump length will be resampled. As we will see, when $P(\tau)$ is heavy-tailed, we obtain the anomalous diffusions with the MSD diffusion exponent in the range 0–2. The diffusion results are shown in Table I. Moreover, we derive the effective jump length density $\lambda_{\mathrm{eff}}(\zeta)$ for the decoupled form and compare it with $P(\tau)$ to help distinguish the diffusion types. When $P(\tau)$ is exponential, the MSD increases linearly with time, but the PDF exhibits a generalized exponential shape at a short time, and after a longer time, it crosses over to a Gaussian shape.

In this paper the numerical calculations are implemented by adopting the Monte Carlo trajectory-simulating technique [52]. The parameters used in the simulations are as follows: the number of trajectories in the ensemble is $\mathrm{N} = 5 \times 10^4$, the time step is $dt = 0.01$, and the total evolution time is $t = 10^5$, which is sufficient for the MSD exponent to converge to a stable value.

III. ANOMALOUS DIFFUSION UNDER A HEAVY-TAILED TIME DENSITY

A. Anomalous diffusive behaviors

We denote $W(x,t)$ as the PDF for the particle to be at x at time t with the initial condition $W(x, t = 0) = \delta(x)$, and $\phi(x,t)$ is the PDF of the particle's position at time t which just finished an instantaneous random jump. Then $\phi(x,t) = \int_{-\infty}^{\infty} dx' \int_0^t dt' \phi(x',t')\psi(x - x', t - t') + \delta(x)\delta(t)$. $\Psi(t) = 1 - \int_0^t P(\tau)\, d\tau$ represents the survival probability, so $W(x,t) = \int_0^t dt' \phi(x,t')\Psi(t-t')$. The Fourier-Laplace representation of $W(x,t)$ is [33]

$$W(k,u) = \frac{1 - P(u)}{u} \frac{1}{1 - \psi(k,u)}, \tag{7}$$

where $\psi(k,u)$ is the transform of $\psi(x,t)$. It is easy to see that $\psi(k,u)|_{k=0} = P(u)$. $\langle x^2(t)\rangle$ can be obtained from calculating $\langle x^n(t)\rangle = i^n \mathscr{L}^{-1}_{u\to t}[\frac{\partial^n}{\partial k^n} W(k,u)]\,|_{k=0}$:

$$\begin{aligned}\langle x^2(t)\rangle &= \mathscr{L}^{-1}_{u\to t}\left\{-\left[\frac{\partial^2}{\partial k^2} W(k,u)\right]\Big|_{k=0}\right\} \\ &= \mathscr{L}^{-1}_{u\to t}\left\{\frac{1-P(u)}{u}\left(\frac{-\psi''(k,u)}{[1-\psi(k,u)]^2}\right.\right. \\ &\quad \left.\left. + \frac{-2[\psi'(k,u)]^2}{[1-\psi(k,u)]^3}\right)\Big|_{k=0}\right\},\end{aligned} \tag{8}$$

where the prime symbols ($'$) and ($''$) signify the first and second derivatives with respect to k, respectively. Note that we consider the unbiased case, which leads $[\psi'(k,u)]|_{k=0}$ to disappear. Considering the joint PDF of a particle from

TABLE I. Values of the MSD diffusion exponents of the coupled model.

$\langle x^2(t)\rangle$	$\sim t^{\alpha+1}$	$0<\sigma<1, -1<\alpha-\sigma<1$
	$\sim t^{\sigma}-\sim t^{\alpha+1}$	$0<\sigma<1, -2<\alpha-\sigma<-1$
	$\sim t^{2+\alpha-\sigma}+\sim t^{3+\alpha-2\sigma}$	$1<\sigma<2, -1<\alpha-\sigma<0$
	$\sim t-\sim t^{2+\alpha-\sigma}+\sim t^{2-\sigma}-\sim t^{3+\alpha-2\sigma}$	$1<\sigma<2, -2<\alpha-\sigma<-1$
	$\sim t+\sim t^{2-\sigma}\sim -t^{1-\sigma}+\sim t^{2+\alpha-\sigma}+\sim t^{3+\alpha-2\sigma}$	$1<\sigma<2, -3<\alpha-\sigma<-2$

Eqs. (1) and (6), we obtain

$$\psi(\zeta,\tau)=\lambda(\zeta|\tau)\,P(\tau)=\frac{1}{\sqrt{2\pi D(\tau)\tau}}\exp\left[-\frac{\zeta^2}{2D(\tau)\tau}\right]\sigma\tau^{-\sigma-1}, \quad (9)$$

in which $D(\tau)\tau=a\tau^{1+\alpha}$.

1. Infinite mean waiting time

The Laplace form of $P(\tau)$ is Eq. (2) in this case. Based on the fact that $\lambda(k|\tau)=\exp(-\frac{1}{2}ak^2\tau^{1+\alpha})$, we expand $\lambda(k|\tau)$ into a Taylor series, and use the Laplace transform for $\psi(k,t)$ to get

$$\psi(k,u)=\mathscr{L}_{\tau\to u}\left[\exp\left(-\tfrac{1}{2}k^2a\tau^{1+\alpha}\right)\sigma\tau^{-\sigma-1}\right]=1-\Omega_\sigma u^\sigma-\tfrac{1}{2}a\sigma k^2\mathscr{L}_{\tau\to u}(\tau^{\alpha-\sigma}). \quad (10)$$

Obviously, $\mathscr{L}_{\tau\to u}(\tau^{\alpha-\sigma})$ determines the expression of $\psi(k,u)$, which needs to be further classified as follows.

For the case $-1<\alpha-\sigma<1$, we use the Tauberian theorem to obtain the expression

$$\mathscr{L}_{\tau\to u}(\tau^{\alpha-\sigma})=\Gamma(\alpha-\sigma+1)u^{\sigma-\alpha-1}. \quad (11)$$

Substituting the result into Eq. (10) and taking the second derivative of $\psi(k,u)$ with respect to k, we obtain

$$[\psi''(k,u)]|_{k=0}=-a\sigma\Gamma(\alpha-\sigma+1)u^{\sigma-\alpha-1}. \quad (12)$$

Substituting this together with $P(u)$ into Eq. (8), we obtain

$$\langle x^2(t)\rangle=\frac{a\sigma\Gamma(\alpha-\sigma+1)}{\Omega_\sigma\Gamma(\alpha+2)}\,t^{\alpha+1}. \quad (13)$$

For the case $-2<\alpha-\sigma<-1$, $\mathscr{L}_{\tau\to u}(\tau^{\alpha-\sigma})$ reads

$$\mathscr{L}_{\tau\to u}(\tau^{\alpha-\sigma})=\frac{1-\Omega_{\sigma-\alpha-1}u^{\sigma-\alpha-1}}{\sigma-\alpha-1}, \quad (14)$$

in which $\Omega_{\sigma-\alpha-1}=|\Gamma(2+\alpha-\sigma)|$. The following calculations are very similar to the procedure of calculating Eq. (12). The corresponding $[\psi''(k,u)]|_{k=0}$ reads

$$[\psi''(k,u)]|_{k=0}=-\frac{a\sigma(1-\Omega_{\sigma-\alpha-1}u^{\sigma-\alpha-1})}{\sigma-\alpha-1}. \quad (15)$$

Substituting this and $P(u)$ into Eq. (8) and applying an inverse Laplace transform yields

$$\langle x^2(t)\rangle=\frac{a}{\Omega_\sigma(\sigma-\alpha-1)\Gamma(\sigma)}\left[t^\sigma-\frac{\Gamma(\sigma+1)\Omega_{\sigma-\alpha-1}}{\Gamma(\alpha+2)}t^{\alpha+1}\right]. \quad (16)$$

For Eq. (13), combined with our previous assumption $-1<\alpha<1$, the MSD diffusion exponent $1+\alpha$ ranges from 0 to 2. For Eq. (16), the right side of the MSD consists of two terms, which means that it corresponds to two diffusion processes. Since diffusion is characterized in the limit of the large timescale $t\to\infty$, when several diffusion terms coexist in the MSD expression, the term with the largest exponent (the first term) dominates the final diffusion result. Numerical simulations are performed to support our analytical results, as shown in Fig. 1 , where Figs. 1(a) and 1(b) represent subdiffusion and superdiffusion corresponding to $-1<\alpha<0$ and $0<\alpha<1$ in Eq. (13), respectively, and Fig. 1(c) corresponds to the case of Eq. (16). It can be seen that since more than one diffusion term coexists, crossover phenomena appear between the diffusion processes in Fig. 1(c). However, the contribution of the small exponential term is quite limited and can affect the diffusion result only at a limited timescale, and the crossover is always followed by a steady state which is characterized by the largest diffusion exponent, just as given in Eq. (16). Crossover phenomena can be observed in various systems as long as there is more than one diffusion process in the evolutions, for example, intracellular transport in biological systems [16], and the transport of granular gases in a homogeneous cooling state or glass-forming liquids [53].

2. Finite mean waiting time

For $1<\sigma<2$, the variance of the jump length is $r^2(\tau)=\int_{-\infty}^{\infty}d\zeta\,\zeta^2\lambda(\zeta|\tau)=a\tau^{\alpha+1}$, so $\tau(r)\simeq r^{\frac{2}{1+\alpha}}$. We do a transform to obtain

$$P(r)\,dr=P[\tau(r)]\left[\frac{d\tau(r)}{dr}\right]dr\simeq r^{-\frac{2\sigma}{1+\alpha}-1}\,dr. \quad (17)$$

Combining this with $P(\tau)\simeq\sigma\tau^{-\sigma-1}$, we find in this case the mean waiting time $\langle\tau\rangle=\int_0^\infty\tau P(\tau)\,d\tau$ is finite. Meanwhile, if $-1<\alpha-\sigma$, $r^2(\tau)$ diverges, which will lead to superdiffusion, while when $\alpha-\sigma<-1$, $r^2(\tau)$ is also finite, the diffusion in this case should be normal Brownian motion. Although this analysis is convenient, we still need to make more detailed calculations, which will show some neglected diffusion phenomena.

The Laplace form of $P(\tau)$ is Eq. (3), and $\psi(k,u)$ is

$$\psi(k,u)=\mathscr{L}_{\tau\to u}\left[\exp\left(-\tfrac{1}{2}k^2a\tau^{1+\alpha}\right)\sigma\tau^{-\sigma-1}\right]=1-\eta_\sigma u+\Omega_\sigma u^\sigma-\tfrac{1}{2}a\sigma k^2\mathscr{L}_{\tau\to u}(\tau^{\alpha-\sigma}). \quad (18)$$

For the case $-1<\alpha-\sigma<1$, we apply a Fourier-Laplace transform to $\psi(\zeta,\tau)$ and combine the result with Eqs. (11) and (18) to obtain

$$[\psi''(k,u)]|_{k=0}=-a\sigma\Gamma(\alpha-\sigma+1)u^{\sigma-\alpha-1}. \quad (19)$$

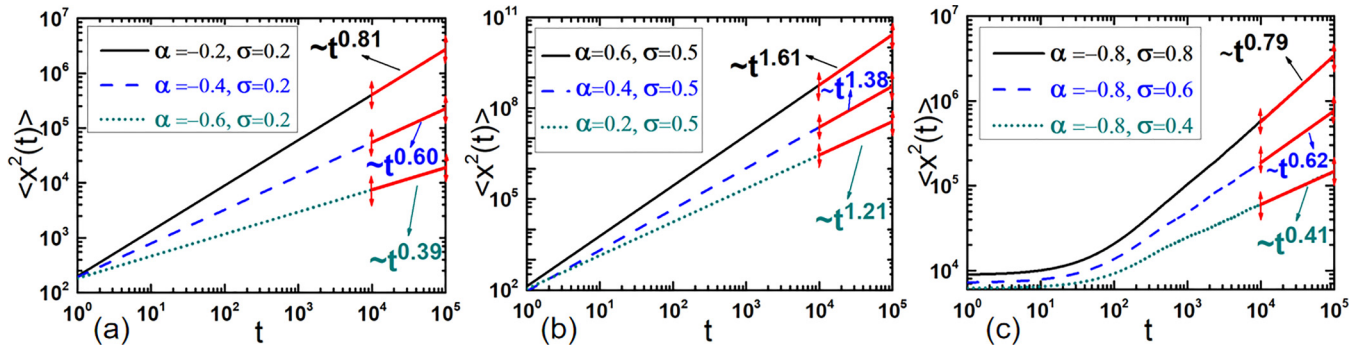

FIG. 1. Simulated plots of $\langle x^2(t)\rangle$ as a function of time t in the case $0 < \sigma < 1$, $-2 < \alpha - \sigma < 1$, represented by the solid black lines, dashed blue lines, and dotted cyan lines, respectively. (a) $-1 < \alpha - \sigma < 1, -1 < \alpha < 0$; (b) $-1 < \alpha - \sigma < 1, 0 < \alpha < 1$; (c) $-2 < \alpha - \sigma < -1$. The solid red lines are the linear fitting results after the evolution curves become steady, executed when $t = 10^4$ in the dimensionless form. The parameter $a = 1.0$ is applied in the three subgraphs. The asymptotic diffusive behaviors agree well with the theoretical predictions.

The corresponding MSD expression is

$$\langle x^2(t)\rangle = \frac{a\sigma\Gamma(\alpha-\sigma+1)}{\eta_\sigma\Gamma(3+\alpha-\sigma)}t^{2+\alpha-\sigma} + \frac{a\sigma\Omega_\sigma\Gamma(\alpha-\sigma+1)}{\eta_\sigma^2\Gamma(4+\alpha-2\sigma)}t^{3+\alpha-2\sigma}. \quad (20)$$

For the case $-2 < \alpha - \sigma < -1$, we combine Eqs. (14) and (18) to obtain the corresponding $[\psi''(k,u)]|_{k=0}$:

$$[\psi''(k,u)]|_{k=0} = -\frac{a\sigma(1-\Omega_{\sigma-\alpha-1}u^{\sigma-\alpha-1})}{\sigma-\alpha-1}. \quad (21)$$

Substituting $[\psi''(k,u)]|_{k=0}$ and $P(u)$ into Eq. (8) yields

$$\langle x^2(t)\rangle = \frac{a\sigma}{(\sigma-\alpha-1)\eta_\sigma}t - \frac{a\sigma\Omega_{\sigma-\alpha-1}}{(\sigma-\alpha-1)\eta_\sigma\Gamma(3+\alpha-\sigma)}t^{2+\alpha-\sigma} + \frac{a\sigma\Omega_\sigma}{(\sigma-\alpha-1)\eta_\sigma^2\Gamma(3-\sigma)}t^{2-\sigma} - \frac{a\sigma\Omega_{\sigma-\alpha-1}\Omega_\sigma}{(\sigma-\alpha-1)\eta_\sigma^2\Gamma(4+\alpha-2\sigma)}t^{3+\alpha-2\sigma}. \quad (22)$$

For the case $-3 < \alpha - \sigma < -2$, $\mathscr{L}_{\tau\to u}(\tau^{\alpha-\sigma})$ can be written as

$$\mathscr{L}_{\tau\to u}(\tau^{\alpha-\sigma}) = \frac{1-\eta_{\sigma-\alpha-1}u+\Omega_{\sigma-\alpha-1}u^{\sigma-\alpha-1}}{\sigma-\alpha-1}, \quad (23)$$

in which $\eta_{\sigma-\alpha-1} = \frac{\sigma-\alpha-1}{\sigma-\alpha-2}$, and $\Omega_{\sigma-\alpha-1} = |\Gamma(2+\alpha-\sigma)|$. The corresponding $[\psi''(k,u)]|_{k=0}$ is given by

$$[\psi''(k,u)]|_{k=0} = -\frac{a\sigma(1-\eta_{\sigma-\alpha-1}u+\Omega_{\sigma-\alpha-1}u^{\sigma-\alpha-1})}{\sigma-\alpha-1}. \quad (24)$$

The MSD expression is

$$\langle x^2(t)\rangle = \frac{a\sigma}{(\sigma-\alpha-1)\eta_\sigma}t - \frac{a\sigma\eta_{\sigma-\alpha-1}}{(\sigma-\alpha-1)\eta_\sigma} + \frac{a\sigma\Omega_{\sigma-\alpha-1}}{(\sigma-\alpha-1)\eta_\sigma\Gamma(3+\alpha-\sigma)}t^{2+\alpha-\sigma} + \frac{a\sigma\Omega_\sigma}{(\sigma-\alpha-1)\eta_\sigma^2\Gamma(3-\sigma)}t^{2-\sigma} - \frac{a\sigma\Omega_\sigma\eta_{\sigma-\alpha-1}}{(\sigma-\alpha-1)\eta_\sigma^2\Gamma(2-\sigma)}t^{1-\sigma} + \frac{a\sigma\Omega_{\sigma-\alpha-1}\Omega_\sigma}{(\sigma-\alpha-1)\eta_\sigma^2\Gamma(4+\alpha-2\sigma)}t^{3+\alpha-2\sigma}. \quad (25)$$

For Eq. (20), the first term of the right side dominates the final diffusion result, producing superdiffusion. For Eqs. (22) and (25), the MSD expressions are similar, both consisting of a term describing normal Brownian motion and several interference terms. Instead of discarding the negligible diffusion terms, we retain all of them to reveal more details. Considering $-3 < \alpha - \sigma < -1$, the MSD grows linearly with time. The numerical simulation results in Fig. 2 confirm our conclusions. Figure 2(a) represents the case of Eq. (20), and Fig. 2(b) represents the case of Eqs. (22) and (25). The diffusion exponents from the numerical simulations are in good agreement with the expected values at large timescales. Note that the crossover phenomena do not appear in Fig. 2(a). The intrinsic reason is although Eq. (20) consists of two diffusion terms, superdiffusion (the first term) is a much more drastic fluctuating stochastic process than subdiffusion (the second term), and thus dominates the whole diffusion process from the beginning and causes the diffusion exponent to steadily show the value of $2+\alpha-\sigma$.

In the cases discussed thus far, it is not difficult to find that the values of parameters α and σ strongly affect the diffusion results. The 3D diagram in Fig. 3 illustrates their competitive relationship well.

B. The role of effective jump length PDF

For the coupled CTRW model, the jump length density$\lambda(\zeta|\tau)$ is given by a Gaussian-like function that is affected by τ. Distinguishing different diffusion types is difficult, so we need a generalized method to solve it. A convenient and intuitive method is to deduce the effective jump length PDF $\lambda_{\rm eff}(\zeta)$ corresponding to the decoupled form. For a decoupled CTRW in which the jump length and waiting time are independent, the joint PDF is $\psi(\zeta,\tau) = \lambda(\zeta)P(\tau)$. We already know that, if the variance of the jump length r^2 diverges, the Lévy distribution

$$\lambda(\zeta) \simeq r^\mu \frac{\Gamma(1+\mu)\sin(\pi\mu/2)}{\pi|\zeta|^{1+\mu}} \quad (26)$$

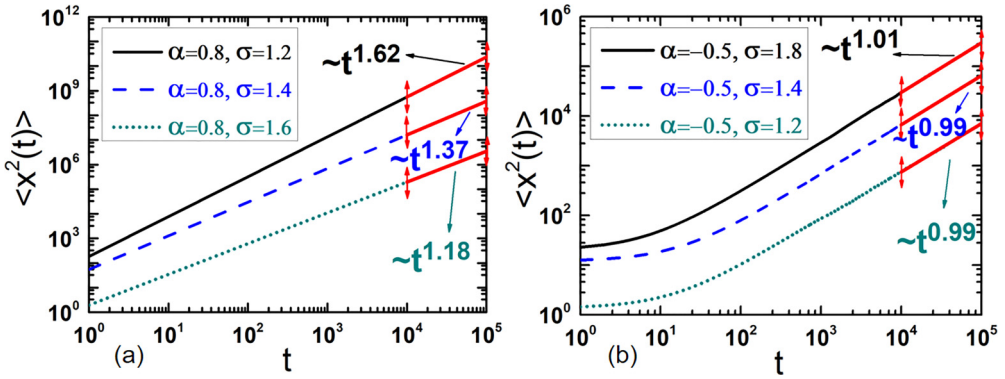

FIG. 2. Simulated plots of $\langle x^2(t)\rangle$ as a function of time t in the case $1 < \sigma < 2$, $-3 < \alpha - \sigma < 1$, represented by lines of different styles and colors. (a) $-1 < \alpha - \sigma < 1$; (b) $-3 < \alpha - \sigma < -1$. The solid red lines are the linear fitting results after the evolution curves become steady, executed when $t = 10^4$ in the dimensionless form. The parameter $a = 1.0$ is applied in the two subgraphs. The asymptotic diffusive behaviors agree well with the theoretical values.

is chosen to be the jump length PDF, which has the form

$$\lambda(k) = \exp(-r^\mu k^\mu) \simeq 1 - r^\mu |k|^\mu, \tag{27}$$

in Fourier space with $1 < \mu < 2$ for small k. When this is combined with $P(\tau) \simeq \sigma\tau^{-\sigma-1}$ in which $0 < \sigma < 1$, the MSD is expressed as [33]

$$\langle x^2(t)\rangle \sim t^{\frac{2\sigma}{\mu}}. \tag{28}$$

The effective jump length PDF $\lambda_{\text{eff}}(\zeta)$ can be calculated from its Fourier form

$$\begin{aligned}\lambda_{\text{eff}}(k) &= \int_0^\infty \psi(k,\tau)\,d\tau = \int_0^\infty \mathscr{F}_{\zeta\to k}[\psi(\zeta,\tau)]d\tau \\ &= \frac{\sigma}{2\pi(\alpha+1)}\int_0^\infty \exp\left(-\frac{1}{2}ak^2\tau^{\alpha+1}\right)\tau^{-\sigma-\alpha-1}\,d\tau^{\alpha+1}.\end{aligned} \tag{29}$$

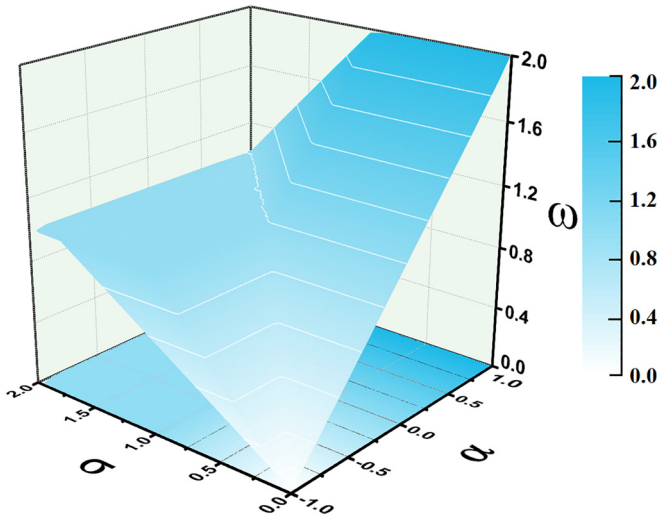

FIG. 3. 3D relationships between σ, α, and ω. The bottom coordinates represent σ and α, whose values range from 0 to 2 and -1 to 1, respectively, and the ordinate represents the diffusion exponent ω. Deeper colors represent larger diffusion exponents, and shallower colors correspond to smaller diffusion exponents.

Equation (29) can be treated as a process for deriving the Laplace form of $f(\tau) = \tau^{-\sigma-\alpha-1}$, where $s = ak^2/2 = a|k|^2/2$ is the transform factor and $\tau^* = \tau^{\alpha+1}$:

$$\begin{aligned}\lambda_{\text{eff}}(k) &= \frac{\sigma}{2\pi(\alpha+1)}\int_0^\infty \exp\left(-\frac{a|k|^2}{2}\tau^*\right)\tau^{*-\frac{\sigma}{\alpha+1}-1}\,d\tau^* \\ &= \frac{\sigma}{2\pi(\alpha+1)}\mathscr{L}_{\tau^*\to\frac{a|k|^2}{2}}\left(\tau^{*-\frac{\sigma}{\alpha+1}-1}\right).\end{aligned} \tag{30}$$

We first consider $0 < \sigma < 1$ and further divide it into two cases for discussion.

For the case $-1 < \alpha - \sigma < 1$,

$$\begin{aligned}&\mathscr{L}_{\tau^*\to\frac{a|k|^2}{2}}\left(\tau^{*-\frac{\sigma}{\alpha+1}-1}\right) \\ &= \frac{\alpha+1}{\sigma}\left[1 - \left|\Gamma\left(1-\frac{\sigma}{\alpha+1}\right)\right|\left(\frac{a}{2}\right)^{\frac{\sigma}{\alpha+1}}|k|^{\frac{2\sigma}{\alpha+1}}\right],\end{aligned} \tag{31}$$

which leads to

$$\lambda_{\text{eff}}(k) = \frac{1}{2\pi}\left[1 - \left|\Gamma\left(1-\frac{\sigma}{\alpha+1}\right)\right|\left(\frac{a}{2}\right)^{\frac{\sigma}{\alpha+1}}|k|^{\frac{2\sigma}{\alpha+1}}\right]. \tag{32}$$

Comparing them with Eqs. (26) and (27), we consider that $r^\mu = |\Gamma(1-\frac{\sigma}{\alpha+1})|(\frac{a}{2})^{\frac{\sigma}{\alpha+1}}$, and $\lambda_{\text{eff}}(\zeta)$ will have a Lévy distribution similar to Eq. (26) with $\mu = \frac{2\sigma}{\alpha+1}$:

$$\lambda_{\text{eff}}(\zeta) \simeq \frac{\left|\Gamma\left(1-\frac{\sigma}{\alpha+1}\right)\right|\left(\frac{a}{2}\right)^{\frac{\sigma}{\alpha+1}}\Gamma\left(1+\frac{2\sigma}{\alpha+1}\right)\sin\left(\pi\frac{\sigma}{\alpha+1}\right)}{2\pi^2|\zeta|^{1+\frac{2\sigma}{\alpha+1}}}. \tag{33}$$

Using $P(\tau) \simeq \sigma\tau^{-\sigma-1}$ and Eq. (28) gives the MSD as

$$\langle x^2(t)\rangle \sim t^{2\sigma/\mu} = t^{2\sigma/\frac{2\sigma}{\alpha+1}} = t^{\alpha+1}, \tag{34}$$

which coincides with Eq. (13).

For the case $-2 < \alpha - \sigma < -1$, a finite τ^* can be obtained from $P(\tau^*) = \tau^{*-\frac{\sigma}{\alpha+1}-1}$, which leads to its Laplace transform approximately equal to $\exp(-\tau^*)$, then

$$\begin{aligned}\lambda_{\text{eff}}(k) &\simeq \frac{\sigma}{2\pi(\alpha+1)}\int_0^\infty \exp\left(-\frac{a|k|^2}{2}\tau^*\right)\exp(-\tau^*)\,d\tau^* \\ &\simeq \frac{\sigma}{2\pi(\alpha+1)}\left(1-\frac{a}{2}|k|^2\right).\end{aligned} \tag{35}$$

This is the Fourier form of the Gaussian distribution, so

$$\langle x^2(t)\rangle \sim t^{2\sigma/2} = t^{\sigma}, \tag{36}$$

which agrees well with Eq. (16). Next, we consider $1 < \sigma < 2$, which also needs to be divided into two cases.

For the case $-1 < \alpha - \sigma < 1$, a finite $\langle\tau\rangle$ can be obtained from $P(\tau) \simeq \sigma\tau^{-\sigma-1}$, which makes its Laplace transform approximately equal to $\exp(-\tau)$. Meanwhile, $\lambda_{\rm eff}(k)$ is the same as in Eq. (32), and the corresponding $\lambda_{\rm eff}(\zeta)$ is given by Eq. (33). Obviously, the corresponding diffusive behavior is superdiffusion, which is consistent with Eq. (20).

For the case $-3 < \alpha - \sigma < -1$, $\lambda_{\rm eff}(k)$ is the same as in Eq. (35). Both r^2 and $\langle\tau\rangle$ are finite, which leads the MSD to exhibit normal diffusion corresponding to Eqs. (22) and (25). It should be noted that when $1 < \sigma < 2$, the MSD cannot be obtained by analogy to Eq. (28), because the prerequisite for its establishment is $0 < \sigma < 1$, which is obviously not satisfied in this case. Certainly, we have to emphasize that distinguishing the diffusion types of a coupled CTRW model has already been discussed in Ref. [54] through a valid computational method, which corresponds to their Eqs. (39a) and (39b), (44a) and (44b), and (47). Our results obtained through $\lambda_{\rm eff}(\zeta)$ are consistent with those in Ref. [54]. However, we still believe that it is necessary to distinguish the diffusion types by deducing the effective jump length PDF $\lambda_{\rm eff}(\zeta)$. Because $\lambda_{\rm eff}(\zeta)$ can indicate that, the property of the present coupled model is essentially equivalent to the competition between a long jump length and a long waiting time. Meanwhile, we note that since all CTRW models are based on the jump length and waiting time, which are depicted by a joint PDF, this approach of distinguishing diffusion types is naturally applicable for other coupled CTRW models.

IV. ANOMALOUS DIFFUSION UNDER AN EXPONENTIAL TIME DENSITY

A. Short time limit

For the heavy-tailed $P(\tau)$ investigated in the previous section, we obtained the anomalous diffusions with the MSD diffusion exponent in the range 0–2 and deduced the effective jump length PDF $\lambda_{\rm eff}(\zeta)$ to distinguish the diffusion types. In this section we present another diffusive behavior, in which the MSD increases linearly with time yet $W(x,t)$ is exponential at a short time, and at longer times, it crosses over to Gaussian.

We choose Eq. (4) as $P(\tau)$ and the power-law relationship between τ and $D(\tau)$ remains unchanged. Granick [55] and Hapca *et al.* [56] have found that the non-Gaussian distribution can be obtained by

$$W(x,t) = \int_0^\infty G(x,t|D)\,P(D)\,dD, \tag{37}$$

where $G(x,t|D)$ is a standard Gaussian distribution

$$G(x,t|D) = \frac{1}{\sqrt{4\pi Dt}}\exp\left(-\frac{x^2}{4Dt}\right) \tag{38}$$

with diffusion coefficient D, and $P(D)$ is the stationary-state probability density of D. This approach corresponds to the superstatistical idea [57]. Tracer particles of a system initially stay alone in disjunct patches with different local diffusion coefficients D, the overall distribution function $W(x,t)$ becomes the weighted average. The superstatistical approach allows us to obtain the non-Gaussian distribution of the particle displacement in the short time limit. In our model, $P(D)$ can be obtained through a proper transform:

$$\begin{aligned} P(D)dD &= P[\tau(D)]\left[\frac{d\tau(D)}{dD}\right]dD \\ &= \left(\frac{1}{a}\right)^{\frac{1}{\alpha}}\frac{1}{\alpha b}D^{\frac{1}{\alpha}-1}\exp\left[-\frac{1}{b}\left(\frac{1}{a}D\right)^{\frac{1}{\alpha}}\right]dD. \end{aligned} \tag{39}$$

When $\alpha = 1.0$, it reduces to $P(D) = \frac{1}{ab}\exp(-\frac{1}{ab}D)$. Substituting it into Eq. (37) and applying the Fourier transform, we obtain

$$W(k,t) = \int_0^\infty P(D)\exp(-k^2Dt)\,dD, \tag{40}$$

where we used the fact that $G(k,t) = \exp(-Dk^2t)$. We assume $s = k^2t$, and then Eq. (40) can be seen as a Laplace transform of $P(D)$:

$$\begin{aligned} W(k,t) &= \int_0^\infty \frac{1}{ab}\exp\left(-\frac{1}{ab}D\right)\exp(-sD)\,dD \\ &= \frac{1}{1+sab} = \frac{1}{1+abk^2t}. \end{aligned} \tag{41}$$

Finally, we take the inverse Fourier transform of $W(k,t)$ to obtain

$$W(x,t) = \frac{1}{\sqrt{4abt}}\exp\left(-\frac{|x|}{\sqrt{abt}}\right), \tag{42}$$

which is a standard Laplace distribution. We can perform the corresponding calculation for the more general case ($\alpha \neq 1.0$). Using the Laplace method, the asymptotic $W(x,t)$ expression exhibits a generalized exponential shape

$$\begin{aligned} W(x,t) \simeq &\frac{\alpha^{\frac{1-\alpha}{2(1+\alpha)}}}{\sqrt{2a(1+\alpha)b^\alpha t}}\left(\frac{|x|}{\sqrt{4ab^\alpha t}}\right)^{\frac{1-\alpha}{1+\alpha}} \\ &\times\exp\left[-(1+\alpha)\alpha^{-\frac{\alpha}{1+\alpha}}\left(\frac{x^2}{4ab^\alpha t}\right)^{\frac{1}{1+\alpha}}\right], \end{aligned} \tag{43}$$

with a power-law prefactor. In particular, the choice $\alpha = 1.0$ leads us back to Eq. (42), which verifies our calculation results. The detailed calculation procedure is given in the Appendix. The MSD can be obtained through Eq. (37) as

$$\begin{aligned} \langle x^2(t)\rangle &= \int_{-\infty}^\infty x^2W(x,t)\,dx \\ &= \int_0^\infty P(D)\int_{-\infty}^\infty x^2G(x,t|D)\,dx\,dD \\ &= 2ab^\alpha\Gamma(2+\alpha)\,t. \end{aligned} \tag{44}$$

We see that the MSD grows linearly with time, yet the $W(x,t)$ of the particle displacement is non-Gaussian and exhibits a generalized exponential profile.

B. Long time limit

After a long time, the particles explore enough patches with different D and a Gaussian distribution with an effective

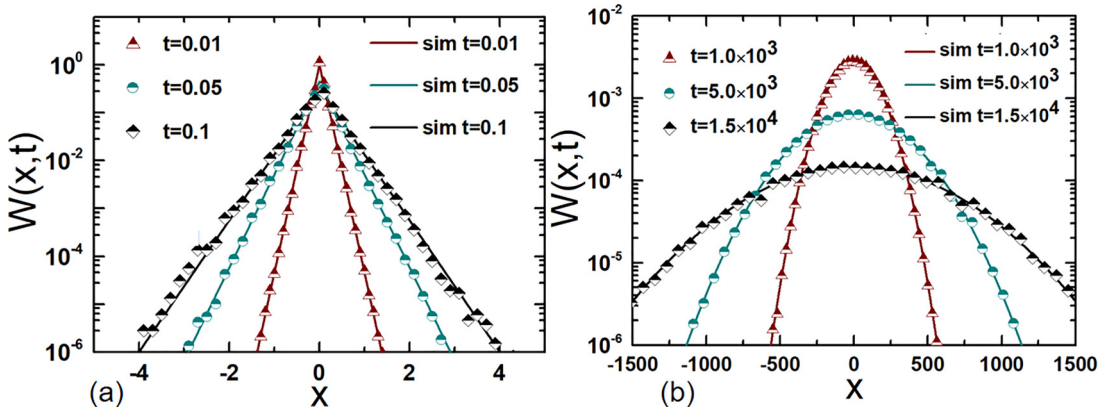

FIG. 4. Dimensionless form of the PDFs $W(x,t)$ at different times, which are represented by the different symbols. (a) Short time limit; (b) long time limit. The different solid lines in the two subgraphs represent the simulation results of Eqs. (43) and (46) at the corresponding times, respectively. The parameters $a = b = \alpha = 1.0$ are applied in these simulations.

diffusion coefficient $\langle D\rangle_{\rm eff}$ emerges, which leads to a standard Brownian motion. Since the superstatistical approach is applicable only in the initial period before the particles begin to jump, in the long time limit, $W(x,t)$ needs to be obtained by Eq. (7). The corresponding $\psi(k,u)$ is expressed as

$$\psi(k,u) = \mathscr{L}_{\tau\to u}\left[\exp\left(-\frac{1}{2}k^2 a\tau^{1+\alpha}\right)\frac{1}{b}\exp\left(-\frac{1}{b}\tau\right)\right]$$
$$= 1 - bu - \frac{1}{2}\Gamma(2+\alpha)ab^{\alpha+1}k. \tag{45}$$

The calculations are similar to the procedure as before, and we directly provide the $W(x,t)$ expression as

$$W(x,t) = \frac{1}{\sqrt{2\pi\langle D\rangle_{\rm eff}t}}\exp\left(-\frac{x^2}{2\langle D\rangle_{\rm eff}t}\right), \tag{46}$$

in which $\langle D\rangle_{\rm eff} = ab^{\alpha}\Gamma(\alpha+2)$. The corresponding MSD expression can be given as

$$\langle x^2(t)\rangle = 2ab^{\alpha}\Gamma(\alpha+2)t, \tag{47}$$

which is consistent with Eq. (44).

By calculating the PDFs and MSDs at different timescales, we found a crossover phenomenon of the PDF, where an initial non-Gaussian distribution is replaced by a Gaussian one. However, the MSD increases linearly with time and is the same in the short time and long time limits. The intrinsic reason is at a short time, all particles are in the waiting period, and are located in different patches with their own local diffusion coefficients D. In this case the ensemble of particles in different patches exhibits a superstatistical behavior. However, at a sufficiently long time, we would not expect the particles to stay in their own local patch forever; once they begin to jump, the assumption of the superstatistical approach will be violated. This means that the first waiting time of particles determines the timescale of the non-Gaussian distribution. The numerical results are shown in Fig. 4. Figures 4(a) and 4(b) show the particle displacement distributions $W(x,t)$ in the short time and long time limits, respectively. Based on the previous results discussed, for the short time distribution $W(x,t)$, we require the timescale $t \ll \langle\tau\rangle$. At this time, most particles are in the waiting period, which can avoid excessive jump events breaking the superstatistical assumption. In the dimensionless case, the particle mean waiting time is $\langle\tau\rangle = \int_0^\infty \tau P(\tau)\,d\tau = 1.0$ according to Eq. (4), which means that $t \ll 1.0$. For a long time, we require the timescale $t \gg 1.0$. Note that although the short timescales we chose are much less than 1.0 as shown in Fig. 4(a), the waiting time τ is obtained by sampling from Eq. (4) rather than a constant, we cannot expect that there are no jump events to occur at the short timescales. Therefore, we claim only that the superstatistical assumption is approximately satisfied in this case. As we can see, when $t = 0.1$, the fitting result is not as good as when $t = 0.01$, indicating that more particles have already occurred to jump at this moment. At a long time, the Gaussian distributions are obtained. In addition, the MSD simulation results are shown Fig. 5. As expected, the MSD is not affected by the crossover between the distribution shapes and increases linearly with time.

In this section we discuss an anomalous diffusive behavior with diffusive characteristics completely different from those in Sec. III. The MSD increases linearly with time, but the PDF $W(x,t)$ of the particle displacement exhibits a generalized exponential shape at a short time, and after a longer time, it crosses over to a Gaussian shape. The diffusion results depend

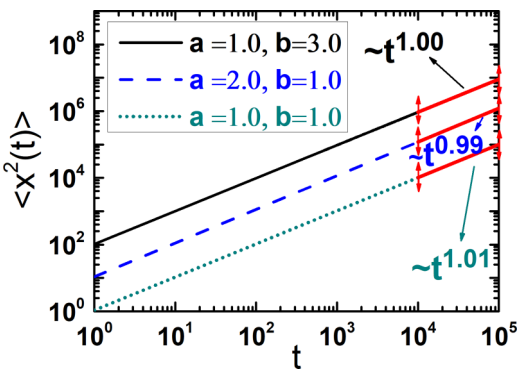

FIG. 5. Simulated plot of $\langle x^2(t)\rangle$ as a function of time t with various a and b. The three parameter sets are $a = 1.0$, $b = 1.0$; $a = 2.0$, $b = 1.0$; and $a = 1.0$, $b = 3.0$, respectively. The solid red lines are the linear fitting results at large timescales, and all agree with the theoretical value of 1.0.

on the form of $P(\tau)$ and the coupling relationship between τ and $D(\tau)$.

Several models have been proposed to explain Brownian yet non-Gaussian diffusion, such as the minimal diffusing diffusivity (DD) model proposed by Chechkin *et al.* [58]. Two models have in common the idea that anomalous diffusive behaviors are a direct consequence of an inhomogeneity of the environment, and both can exhibit a crossover from non-Gaussian to standard Gaussian processes. However, they describe completely different physical scenarios. Our model describes a static environment with sharp boundaries between regions with different D, whereas in the minimal DD model, the instantaneous diffusion coefficients of particles in patches change gradually, which physically corresponds to a slowly changing dynamic environment. Meanwhile, in the minimal DD model, anomalous diffusions originate from the common motion of particles and the environment, whereas in our model, anomalous diffusions originate only from the motion of particles themselves. Therefore, both the environment studied and the diffusion mechanisms are different and need to be distinguished.

V. CONCLUSION

Anomalous diffusions in inhomogeneous environments have been extensively studied in recent years, especially in intracellular media, which typically exhibit various diffusive behaviors. In this paper we develop a coupled CTRW model in which the waiting time τ is associated with the local environmental diffusion coefficient $D(\tau)$ through a power-law coupling to demonstrate the environmental inhomogeneities. We provide two forms of the waiting time density $P(\tau)$, and the corresponding jump length density $\lambda(\zeta|\tau)$ is defined by a Gaussian-like function. The numerical and analytical results indicate that when $P(\tau)$ is heavy-tailed, the particles exhibit the anomalous diffusions with the diffusion exponent between 0 and 2. The MSD expression consists of several diffusion terms and is dominated by the largest exponential term. When $P(\tau)$ is exponential, the MSD increases linearly with time yet the PDF $W(x,t)$ of particle displacement has a generalized exponential shape at a short time, and at a longer time, it crosses over to a Gaussian profile, which is consistent with experimental results [43–46]. In addition, for the multiple diffusion types in Sec. III, we deduce the effective jump length PDF $\lambda_{\rm eff}(\zeta)$ corresponding to the decoupled case to help distinguish the diffusion types. $\lambda_{\rm eff}(\zeta)$ indicates that the present coupled model is essentially equivalent to the competition between a long jump length and a long waiting time. This approach of distinguishing diffusion types is also applicable for other coupled CTRW models. In terms of the results, we successfully explain two kinds of anomalous diffusive behavior with different characteristics. Since they occur in the same environment, there should be the similarity [the coupling relationship between $D(\tau)$ and τ] and the difference [the form of $P(\tau)$] in the model.

The superstatistical idea has been widely used in a variety of complex systems in recent years. For example, superstatistical Brownian motion is applied to describe some soft matter and biological systems with two statistical levels, which present a crossover phenomenon from a non-Gaussian distribution to standard Gaussian distribution [58,59], and a two-variable superstatistical formalism is developed and applied to describe the stochastic motion of histonelike nucleoid-structuring proteins in living *E. coli* bacteria [60], among other examples [61–65]. Our future work will attempt to apply the superstatistical idea to solve more diffusion phenomena observed in experiments. We believe that the coupled CTRW model developed in this paper has potential applications in describing anomalous diffusive behaviors in inhomogeneous environments.

ACKNOWLEDGMENT

This work was supported by the National Natural Science Foundation of China under Grant No. 12347212.

APPENDIX: CALCULATING THE INTEGRAL OF EQ. (37) VIA THE LAPLACE METHOD FOR THE CASE OF $\alpha \neq 1.0$

The asymptotic behavior of $W(x,t)$ can generally be obtained by using the Laplace method. We know that $W(x,t)$ can be obtained via

$$\begin{aligned} W(x,t) &= \int_0^\infty P(D)\, P(x,t|D)\, dD \\ &= \frac{\left(\frac{1}{a}\right)^{\frac{1}{\alpha}} \frac{1}{\alpha b}}{\sqrt{4\pi t}} \int_0^\infty D^{\frac{1}{\alpha}-\frac{3}{2}} \exp\left[-\left(\frac{1}{ab^\alpha} D\right)^{\frac{1}{\alpha}} \right] \\ &\quad \times \exp\left(-\frac{x^2}{4Dt} \right) dD, \end{aligned} \tag{A1}$$

where we set $\lambda = \frac{x^2}{4ab^\alpha t}$. Changing the variable of integration to $y = \frac{D}{ab^\alpha}$ yields

$$W(x,t) = \frac{\left(\frac{1}{a}\right)^{\frac{1}{\alpha}} \frac{1}{\alpha b}}{\sqrt{4\pi t}} \int_0^\infty (ab^\alpha y)^{\frac{1}{\alpha}-\frac{3}{2}} \exp\left(-y^{\frac{1}{\alpha}} - \lambda/y \right) ab^\alpha\, dy. \tag{A2}$$

Setting $\tilde{D} = y^{-1}$ and rearranging gives

$$W(x,t) = \frac{1}{\sqrt{4\pi ab^\alpha t \alpha^2}} \int_0^\infty \tilde{D}^{-\frac{1}{2}-\frac{1}{\alpha}} \exp\left(-\tilde{D}^{-\frac{1}{\alpha}} - \lambda\tilde{D} \right) d\tilde{D}. \tag{A3}$$

This can be regarded as an integral Laplace form:

$$\Delta = \int_0^\infty f(\tilde{D}) \exp(-\lambda\tilde{D})\, d\tilde{D}. \tag{A4}$$

Note that the Laplace method can be used only in the case $f(0) \neq 0$. Obviously, our case $f(0) = 0$ together with all its derivatives is not applicable. Thus, in order to evaluate the asymptotics, we define the maximum of the function

$$\phi(\tilde{D}) = -\lambda\tilde{D} - \tilde{D}^{-\frac{1}{\alpha}}. \tag{A5}$$

This can be obtained by taking the derivative

$$\begin{aligned} \frac{d\phi(\tilde{D})}{d\tilde{D}} &= -\lambda + \frac{1}{\alpha}\tilde{D}^{-\frac{1}{\alpha}-1} = 0, \\ \tilde{D}_{\max} &= (\lambda\alpha)^{-\frac{\alpha}{1+\alpha}}. \end{aligned} \tag{A6}$$

We introduce a variable $t = \tilde{D}/\tilde{D}_{\max}$, such that Eq. (A4) becomes

$$\begin{aligned}\Delta &= \int_0^\infty \tilde{D}^{-\frac{1}{2}-\frac{1}{\alpha}} \exp\left(-\tilde{D}^{-\frac{1}{\alpha}} - \lambda\tilde{D}\right) d\tilde{D} \\ &= (\lambda\alpha)^{\frac{2-\alpha}{2(1+\alpha)}} \int_0^\infty t^{-\frac{1}{2}-\frac{1}{\alpha}} \exp\Big[\Big(-\lambda^{\frac{1}{1+\alpha}}\Big) \\ &\quad \times \left(t^{-\frac{1}{\alpha}}\alpha^{\frac{1}{1+\alpha}} + t\alpha^{-\frac{\alpha}{1+\alpha}}\right)\Big] dt. \end{aligned} \tag{A7}$$

We set $\tilde{\lambda} = \lambda^{\frac{1}{1+\alpha}}$ and $\Omega = t\,\alpha^{-\frac{\alpha}{1+\alpha}}$ at the same time. Then Eq. (A7) becomes

$$\begin{aligned}\Delta = \lambda^{\frac{2-\alpha}{2(1+\alpha)}} &\int_0^\infty \Omega^{-\frac{\alpha+2}{2\alpha}} \\ &\times \exp\left[\tilde{\lambda} \times \left(-\Omega - \Omega^{-\frac{1}{\alpha}}\right)\right] d\Omega. \end{aligned} \tag{A8}$$

We set the function $S(\Omega) = -\Omega - \Omega^{-\frac{1}{\alpha}}$, and then the Laplace method can be used in Eq. (A8). The function $S(\Omega)$ reaches its maximum at $\Omega_{\max} = \alpha^{-\frac{\alpha}{1+\alpha}}$. We take the result into $S(\Omega)$ to get

$$S(\Omega_{\max}) = -(1+\alpha)\alpha^{-\frac{\alpha}{1+\alpha}}. \tag{A9}$$

Meanwhile, we compute the second derivative of $S(\Omega)$ as

$$S''(\Omega_{\max}) = -\frac{1}{\alpha}\left(1+\frac{1}{\alpha}\right)\alpha^{\frac{1+2\alpha}{1+\alpha}}. \tag{A10}$$

We can substitute the results into Eq. (A8) to get the expression

$$\begin{aligned}\Delta &= \lambda^{\frac{2-\alpha}{2(1+\alpha)}} \int_0^\infty \Omega^{-\frac{\alpha+2}{2\alpha}} \exp[\tilde{\lambda}S(\Omega)]\, d\Omega \\ &\simeq \lambda^{\frac{2-\alpha}{2(1+\alpha)}} \int_{\Omega_{\max}-\epsilon}^{\Omega_{\max}+\epsilon} \Omega^{-\frac{\alpha+2}{2\alpha}} \exp\left[\tilde{\lambda}\left(S(\Omega_{\max}) \right.\right. \\ &\quad \left.\left. + \frac{(\Omega-\Omega_{\max})^2}{2} S''(\Omega_{\max})\right)\right] d\Omega \\ &\simeq \lambda^{\frac{2-\alpha}{2(1+\alpha)}}\, \Omega_{\max}^{-\frac{\alpha+2}{2\alpha}} \exp[\tilde{\lambda}S(\Omega_{\max})] \\ &\quad \times \int_{-\infty}^{\infty} \exp\left[-\frac{\tilde{\lambda}}{2}|S''(\Omega_{\max})|\Omega^2\right] d\Omega \\ &= \lambda^{\frac{2-\alpha}{2(1+\alpha)}}\, \Omega_{\max}^{-\frac{\alpha+2}{2\alpha}} \exp[\tilde{\lambda}S(\Omega_{\max})] \sqrt{\frac{2\pi}{\tilde{\lambda}|S''(\Omega_{\max})|}} \\ &= \left(\frac{|x|}{\sqrt{4ab^\alpha t}}\right)^{\frac{1-\alpha}{1+\alpha}} \frac{\sqrt{2\pi}\alpha}{\sqrt{1+\alpha}}\, \alpha^{\frac{1-\alpha}{2(1+\alpha)}} \\ &\quad \times \exp\left[-(1+\alpha)\alpha^{-\frac{\alpha}{1+\alpha}}\left(\frac{x^2}{4ab^\alpha t}\right)^{\frac{1}{1+\alpha}}\right]. \end{aligned} \tag{A11}$$

Finally, bringing the previous coefficient into Eq. (A11), we have the following approximate result for $W(x,t)$:

$$\begin{aligned}W(x,t) \simeq \frac{\alpha^{\frac{1-\alpha}{2(1+\alpha)}}}{\sqrt{2a(1+\alpha)b^\alpha t}} &\left(\frac{|x|}{\sqrt{4ab^\alpha t}}\right)^{\frac{1-\alpha}{1+\alpha}} \\ &\times \exp\left[-(1+\alpha)\alpha^{-\frac{\alpha}{1+\alpha}}\left(\frac{x^2}{4ab^\alpha t}\right)^{\frac{1}{1+\alpha}}\right]. \end{aligned} \tag{A12}$$

[1] R. Brown, A brief account of microscopical observations made on the particles contained in the pollen of plants, Phil. Mag. **4**, 161 (1828).

[2] J. Perrin, Mouvement brownien et réalité moléculaire, Ann. Chim. Phys. **18**, 5 (1909).

[3] I. Nordlund, Eine neue bestimmung der avogadroschen konstante aus der brownschen bewegung kleiner, in wasser suspendierten quecksilberkügelchen, Z. Phys. Chem. **87U**, 40 (1914).

[4] E. Kappler, Versuche zur Messung der avogadro-loschmidtschen Zahl aus der brownschen Bewegung einer Drehwaage, Ann. Phys. **403**, 233 (1931).

[5] A. Einstein, Über die von der molekularkinetischen Theorie der wärme geforderte Bewegung von in ruhenden Flüssigkeiten suspendierten Teilchen, Ann. Phys. **322**, 549 (1905).

[6] W. Sutherland, LXXV. A dynamical theory of diffusion for non-electrolytes and the molecular mass of albumin, Phil. Mag. **9**, 781 (1905).

[7] M. von Smoluchowski, Zur kinetischen Theorie der brownschen Molekularbewegung und der Suspensionen, Ann. Phys. **326**, 756 (1906).

[8] D. S. Lemons and A. Gythiel, Paul langevin's 1908 paper "On the theory of Brownian Motion" ["Sur la théorie du mouvement brownien," C. R. Acad. Sci. (Paris) **146**, 530 (1908)], Am. J. Phys. **65**, 1079 (1997).

[9] D. Sherrington, Stochastic processes in physics and chemistry, Phys. Bull. **34**, 166 (1983).

[10] J.-B. Masson, P. Dionne, C. Salvatico, M. Renner, C. G. Specht, A. Triller, and M. Dahan, Mapping the energy and diffusion landscapes of membrane proteins at the cell surface using high-density single-molecule imaging and Bayesian inference: Application to the multiscale dynamics of glycine receptors in the neuronal membrane, Biophys. J. **106**, 74 (2014).

[11] J.-P. Bouchaud and A. Georges, Anomalous diffusion in disordered media: Statistical mechanisms, models and physical applications, Phys. Rev. **195**, 127 (1990).

[12] R. Metzler and J. Klafter, The random walk's guide to anomalous diffusion: A fractional dynamics approach, Phys. Rev. **339**, 1 (2000).

[13] R. Metzler and J. Klafter, The restaurant at the end of the random walk: Recent developments in the description of anomalous transport by fractional dynamics, J. Phys. A **37**, R161 (2004).

[14] R. Metzler, J.-H. Jeon, A. G. Cherstvy, and E. Barkai, Anomalous diffusion models and their properties: Non-stationarity, non-ergodicity, and ageing at the centenary of single particle tracking, Phys. Chem. Chem. Phys. **16**, 24128 (2014).

[15] R. Metzler, J.-H. Jeon, and A. G. Cherstvy, Non-Brownian diffusion in lipid membranes: Experiments and simulations, Biochim. Biophys. Acta Biomembranes **1858**, 2451 (2016).
[16] F. Höfling and T. Franosch, Anomalous transport in the crowded world of biological cells, Rep. Prog. Phys. **76**, 046602 (2013).
[17] K. Norregaard, R. Metzler, C. M. Ritter, K. Berg-Sørensen, and L. B. Oddershede, Manipulation and motion of organelles and single molecules in living cells, Chem. Rev. **117**, 4342 (2017).
[18] J.-H. Jeon, V. Tejedor, S. Burov, E. Barkai, C. Selhuber-Unkel, K. Berg-Sørensen, L. Oddershede, and R. Metzler, *In vivo* anomalous diffusion and weak ergodicity breaking of lipid granules, Phys. Rev. Lett. **106**, 048103 (2011).
[19] S. A. Tabei, S. Burov, H. Y. Kim, A. Kuznetsov, T. Huynh, J. Jureller, L. H. Philipson, A. R. Dinner, and N. F. Scherer, Intracellular transport of insulin granules is a subordinated random walk, Proc. Natl. Acad. Sci. USA **110**, 4911 (2013).
[20] C. Di Rienzo, V. Piazza, E. Gratton, F. Beltram, and F. Cardarelli, Probing short-range protein Brownian motion in the cytoplasm of living cells, Nat. Commun. **5**, 5891 (2014).
[21] D. S. Banks and C. Fradin, Anomalous diffusion of proteins due to molecular crowding, Biophys. J. **89**, 2960 (2005).
[22] J. Szymanski and M. Weiss, Elucidating the origin of anomalous diffusion in crowded fluids, Phys. Rev. Lett. **103**, 038102 (2009).
[23] J.-H. Jeon, N. Leijnse, L. B. Oddershede, and R. Metzler, Anomalous diffusion and power-law relaxation of the time averaged mean squared displacement in worm-like micellar solutions, New J. Phys. **15**, 045011 (2013).
[24] G. R. Kneller, K. Baczynski, and M. Pasenkiewicz-Gierula, Communication: Consistent picture of lateral subdiffusion in lipid bilayers: Molecular dynamics simulation and exact results, J. Chem. Phys. **135**, 141105 (2011).
[25] S. Stachura and G. R. Kneller, Communication: Probing anomalous diffusion in frequency space, J. Chem. Phys. **143**, 191103 (2015).
[26] J.-H. Jeon, Hector Martinez-Seara Monne, M. Javanainen, and R. Metzler, Anomalous diffusion of phospholipids and cholesterols in a lipid bilayer and its origins, Phys. Rev. Lett. **109**, 188103 (2012).
[27] J.-H. Jeon, M. Javanainen, H. Martinez-Seara, R. Metzler, and I. Vattulainen, Protein crowding in lipid bilayers gives rise to non-Gaussian anomalous lateral diffusion of phospholipids and proteins, Phys. Rev. X **6**, 021006 (2016).
[28] T. Akimoto, E. Yamamoto, K. Yasuoka, Y. Hirano, and M. Yasui, Non-Gaussian fluctuations resulting from power-law trapping in a lipid bilayer, Phys. Rev. Lett. **107**, 178103 (2011).
[29] A. Caspi, R. Granek, and M. Elbaum, Enhanced diffusion in active intracellular transport, Phys. Rev. Lett. **85**, 5655 (2000).
[30] D. Robert, T.-H. Nguyen, F. Gallet, and C. Wilhelm, In vivo determination of fluctuating forces during endosome trafficking using a combination of active and passive microrheology, PLoS ONE **5**, e10046 (2010).
[31] E. W. Montroll and G. H. Weiss, Random walks on lattices. II, J. Math. Phys. **6**, 167 (1965).
[32] H. Scher and E. W. Montroll, Anomalous transit-time dispersion in amorphous solids, Phys. Rev. B **12**, 2455 (1975).
[33] J. Klafter and I. M. Sokolov, *First Steps in Random Walks: From Tools to Applications* (Oxford University Press, Oxford, 2011).
[34] A. Sergé, N. Bertaux, H. Rigneault, and D. Marguet, Dynamic multiple-target tracing to probe spatiotemporal cartography of cell membranes, Nat. Methods **5**, 687 (2008).
[35] B. P. English, V. Hauryliuk, A. Sanamrad, S. Tankov, N. H. Dekker, and J. Elf, Single-molecule investigations of the stringent response machinery in living bacterial cells, Proc. Natl. Acad. Sci. USA **108**, E365 (2011).
[36] T. Kühn, T. O. Ihalainen, J. Hyväluoma, N. Dross, S. F. Willman, J. Langowski, M. Vihinen-Ranta, and J. Timonen, Protein diffusion in mammalian cell cytoplasm, PLoS ONE **6**, e22962 (2011).
[37] P. J. Cutler, M. D. Malik, S. Liu, J. M. Byars, D. S. Lidke, and K. A. Lidke, Multi-color quantum dot tracking using a high-speed hyperspectral line-scanning microscope, PLoS ONE **8**, e64320 (2013).
[38] G. Giannone, E. Hosy, J.-B. Sibarita, D. Choquet, and L. Cognet, High-content super-resolution imaging of live cell by uPAINT, in *Nanoimaging*, Methods in Molecular Biology, Vol. 950, edited by A. Sousa and M. Kruhlak (Humana Press, Totowa, NJ, 2013), pp. 95–110.
[39] I. Golding and E. C. Cox, Physical nature of bacterial cytoplasm, Phys. Rev. Lett. **96**, 098102 (2006).
[40] S. C. Weber, A. J. Spakowitz, and J. A. Theriot, Bacterial chromosomal loci move subdiffusively through a viscoelastic cytoplasm, Phys. Rev. Lett. **104**, 238102 (2010).
[41] A. V. Weigel, B. Simon, M. M. Tamkun, and D. Krapf, Ergodic and nonergodic processes coexist in the plasma membrane as observed by single-molecule tracking, Proc. Natl. Acad. Sci. USA **108**, 6438 (2011).
[42] J. F. Reverey, J.-H. Jeon, H. Bao, M. Leippe, R. Metzler, and C. Selhuber-Unkel, Superdiffusion dominates intracellular particle motion in the supercrowded cytoplasm of pathogenic *Acanthamoeba castellanii*, Sci. Rep. **5**, 11690 (2015).
[43] T. Toyota, D. A. Head, C. F. Schmidt, and D. Mizuno, Non-Gaussian athermal fluctuations in active gels, Soft Matter **7**, 3234 (2011).
[44] M. T. Valentine, P. D. Kaplan, D. Thota, J. C. Crocker, T. Gisler, R. K. Prud'homme, M. Beck, and D. A. Weitz, Investigating the microenvironments of inhomogeneous soft materials with multiple particle tracking, Phys. Rev. E **64**, 061506 (2001).
[45] M. S. e Silva, B. Stuhrmann, T. Betz, and G. H. Koenderink, Time-resolved microrheology of actively remodeling actomyosin networks, New J. Phys. **16**, 075010 (2014).
[46] N. Samanta and R. Chakrabarti, Tracer diffusion in a sea of polymers with binding zones: Mobile vs. frozen traps, Soft Matter **12**, 8554 (2016).
[47] P. Massignan, C. Manzo, J. A. Torreno-Pina, M. F. García-Parajo, M. Lewenstein, and G. J. Lapeyre Jr., Nonergodic subdiffusion from Brownian motion in an inhomogeneous medium, Phys. Rev. Lett. **112**, 150603 (2014).
[48] A. I. Saichev and S. G. Utkin, Random walks with intermediate anomalous-diffusion asymptotics, J. Exp. Theor. Phys. **99**, 443 (2004).
[49] E. Barkai and S. Burov, Packets of diffusing particles exhibit universal exponential tails, Phys. Rev. Lett. **124**, 060603 (2020).
[50] S. Vitali, P. Paradisi, and G. Pagnini, Anomalous diffusion originated by two Markovian hopping-trap mechanisms, J. Phys. A: Math. Theor. **55**, 224012 (2022).

[51] V. Zaburdaev, S. Denisov, and J. Klafter, Lévy walks, Rev. Mod. Phys. **87**, 483 (2015).

[52] E. Heinsalu, M. Patriarca, I. Goychuk, G. Schmid, and P. Hänggi, Fractional Fokker-Planck dynamics: Numerical algorithm and simulations, Phys. Rev. E **73**, 046133 (2006).

[53] A. Bodrova, A. K. Dubey, S. Puri, and N. Brilliantov, Intermediate regimes in granular Brownian motion: Superdiffusion and subdiffusion, Phys. Rev. Lett. **109**, 178001 (2012).

[54] M. F. Shlesinger, J. Klafter, and Y. M. Wong, Random walks with infinite spatial and temporal moments, J. Stat. Phys. **27**, 499 (1982).

[55] B. Wang, J. Kuo, S. C. Bae, and S. Granick, When Brownian diffusion is not Gaussian, Nat. Mater. **11**, 481 (2012).

[56] S. Hapca, J. W. Crawford, and I. M. Young, Anomalous diffusion of heterogeneous populations characterized by normal diffusion at the individual level, J. R. Soc. Interface **6**, 111 (2009).

[57] C. Beck, Dynamical foundations of nonextensive statistical mechanics, Phys. Rev. Lett. **87**, 180601 (2001).

[58] A. V. Chechkin, F. Seno, R. Metzler, and I. M. Sokolov, Brownian yet non-Gaussian diffusion: From superstatistics to subordination of diffusing diffusivities, Phys. Rev. X **7**, 021002 (2017).

[59] E. B. Postnikov, A. Chechkin, and I. M. Sokolov, Brownian yet non-Gaussian diffusion in heterogeneous media: From superstatistics to homogenization, New J. Phys. **22**, 063046 (2020).

[60] Y. Itto and C. Beck, Superstatistical modelling of protein diffusion dynamics in bacteria, J. R. Soc. Interface **18**, 20200927 (2021).

[61] M. A. F. dos Santos, E. H. Colombo, and C. Anteneodo, Random diffusivity scenarios behind anomalous non-Gaussian diffusion, Chaos Solitons & Fractals **152**, 111422 (2021).

[62] D. Molina-García, T. M. Pham, P. Paradisi, C. Manzo, and G. Pagnini, Fractional kinetics emerging from ergodicity breaking in random media, Phys. Rev. E **94**, 052147 (2016).

[63] M. A. F. dos Santos and L. M. Junior, Random diffusivity models for scaled Brownian motion, Chaos Solitons Fractals **144**, 110634 (2021).

[64] A. Maćkała and M. Magdziarz, Statistical analysis of superstatistical fractional Brownian motion and applications, Phys. Rev. E **99**, 012143 (2019).

[65] R. Metzler, Superstatistics and non-Gaussian diffusion, Eur. Phys. J. Spec. Top. **229**, 711 (2020).